

# OPTIMIZING PARAMETERS FOR CUTTING POWER AND SURFACE ROUGHNESS IN VAT 80A<sup>®</sup> TURNING WITH EXPERIMENTAL AL<sub>2</sub>O<sub>3</sub>-MGO CERAMIC TOOL

**Raphael Augusto de Oliveira Santos**

**Prof. Dr. Marcos Valerio Ribeiro**

**Prof. Dr. Manoel Cleber de Sampaio Alves**

Universidade Estadual Paulista – UNESP, Câmpus de Guaratinguetá.

Av. Ariberto Pereira da Cunha, 333 - Portal das Colinas - Guaratinguetá/SP - CEP 12.516-410

raphael.santos@unesp.br

marcos.valerio@unesp.br

manoel.alves@unesp.br

**Abstract.** *The objective of this research was to study the machining of the superalloy VAT 80A<sup>®</sup> using an experimental alumina-based ceramic tool. The factors in this study were the cutting speed, feed, and the depth of cut, and the responses were the cutting power and the surface roughness of the workpiece. A full factorial design was used, and the analysis of variance was employed to determine the optimal parameters. The optimal parameters found in this paper was  $v_c = 400$  m/min,  $f = 0.15$  mm/rev and  $a_p = 0.15$  m. The tests showed the viability of using the experimental ceramic tool in the turning of the VAT 80A<sup>®</sup>.*

**Keywords:** *ceramic tool, nickel-based superalloy, turning, cutting power, roughness*

## 1. INTRODUCTION

The term superalloy describes a variety of metals based on nickel, nickel-iron, or cobalt that exhibits a combination of mechanical strength and resistance to surface degradation. Superalloys are primarily used in aerospace, nuclear, marine, chemical and automobile industries in components such as aircraft gas turbines, steam turbines from power plants and nuclear power system. (Thakur and Gangopadhyay, 2015).

The superalloy VAT 80A<sup>®</sup> is a nickel-based superalloy that was developed by the Villares Metals based on the composition of the superalloy Nimonic 80A. One of its most common uses is to manufacture high performance internal combustion engines. On the Table 1 it is found the nominal chemical composition of the superalloy VAT 80A<sup>®</sup>.

Table 1. Nominal chemical composition of the superalloy VAT 80A<sup>®</sup>. (Farina, *et al.* 2013)

C	Si	Mn	Ni	Nb	Al	Ti	Cr	Fe
0.02	0.20	0.30	Balance	--	1.50	2.20	20.00	0.30

Due to their high properties, the machining of superalloys has shown great difficulties. Among them are the high resistance, hot hardness, high dynamic shear strength, high abrasiveness caused by the presence of hard carbides in their microstructure, low thermal conductivity and chemical affinity with the alloy elements. (Chondhury, 1998, and Ezugwu, 2005)

The use of ceramic tools in the machining of superalloys have been studied by many researchers like Vishwanath *et al* (2019) who studied the use of an alumina based ceramic tool in the turning process of the superalloy Nimonic 80A; and the works of Bonhin, *et al.* (2019) and Kondo, *et al.* (2019) that employed an experimental ceramic tool based on Al<sub>2</sub>O<sub>3</sub>-MgO in the turning process of the superalloy VAT 32<sup>®</sup>.

The main goal of this work is the optimization of the cutting parameters in the turning process of the superalloy VAT 80A<sup>®</sup> using an experimental Al<sub>2</sub>O<sub>3</sub>-MgO-based ceramic tool. The cutting parameters analyzed were the cutting speed, the feed and the depth of cut. The responses were the cutting power and the surface roughness  $R_a$  and  $R_t$  of the workpiece.

## 2. MATERIALS AND METHODS

### 2.1 Workpiece

The material used in this work was the superalloy VAT 80A<sup>®</sup>, donated by Villares Metals SA, located in Brazil, measuring initially 86 mm of diameter and 228 mm of length. The material was provided in the same condition that is used in the industries, that is, after a solution and aging treatments.

## 2.2 Tool's material and characteristics

The tools used in this paper were developed by “Grupo de Pesquisas do Laboratório de Estudo da Usinagem – Faculdade de Engenharia de Guaratinguetá”. They were made of Alumina  $\alpha$  dust and magnesium oxide, 97.75% and 0.25 % in weight, respectively. On the Table 2 it shows some properties from the tool.

Table 2. Properties of the ceramic tool. (Sousa, 2020)

Property	Value
Relative Density (%)	98.25
Hardness (GPa)	14.16
$KIc$ (MPa.m <sup>1/2</sup> )	2.13 $\pm$ 0.25

The experimental ceramic tool has the shape of a square of 12.76 mm width, rake angle  $\gamma$  of 20°, nose radius of 0.8 mm and no chip breaker. The process to produce it was carry out by the authors and can be found in Souza (2020). The tool holder used in this paper is the model CAPTO B01T9032445 from SECO TOOLS<sup>™</sup>.

## 2.3 Signal Acquisition

This study was done in the Laboratório de Estudos da Usinagem – Faculdade de Engenharia de Guaratinguetá. To perform the tests in this study, the machining process was made in a machining center CNC ROMI<sup>™</sup> model GL240M with 15 kW of power. A power transformer model AT 50 B10 from LEM<sup>™</sup> which picks up the electric current directly from the input of the motor that drives the spindle. A BNC-2120 channel module from National Instruments<sup>™</sup> was connect to a computer with a data acquisition board, from the same company. Using the power sensor, the response of cutting power was recorded using the software LABVIEW<sup>®</sup>, also National Instruments<sup>™</sup>. The signal was recorded in power value (V) and it needed to be converted to the unit of cutting power (W). All data was recorded using 4000 points per second of acquisition rate and it was posteriority filtered and processed in a routine developed in the software MATLAB<sup>®</sup>.

The surface roughness was obtained with a roughness meter model MarSuf M300 + RD18 from Mahr according to standard ABNT NBR ISO 4288:2008- Geometrical product specifications (GPS) - Surface texture: Profile method - Rules and procedures for the assessment of surface texture with a cut-off of 0.8mm.

## 2.4 Design of experiments

In this paper, it was taken in consideration the full factorial design of experiments with three factors and two levels each (2<sup>3</sup>). The factors selected for this analysis were the cutting speed ( $v_c$ ), the feed ( $f$ ) and the depth of cut ( $a_p$ ). The responses were the cutting power and the surface roughness of the workpiece. Each combination of parameters was tested three times, totalizing 24 tests of these analysis. On the Table 3 it shows the levels of each factor.

Table 3 – Machining parameter and their levels.

Factor	Low	High
Cutting speed “ $v_c$ ” (m/min)	300	400
Feed “ $f$ ” (mm/rev)	0.15	0.30
Depth of cut $a_p$ (mm)	0.15	0.30

It was made an analysis of variance, ANOVA, to understand how the factors affect the responses. The statistical analysis was done using the software MINITAB<sup>®</sup>.

## 3. RESULTS AND DISCUSSION

### 3.1 Cutting power

On Figure 1 it is found the main effects of the factors in the response of cutting power, in W.

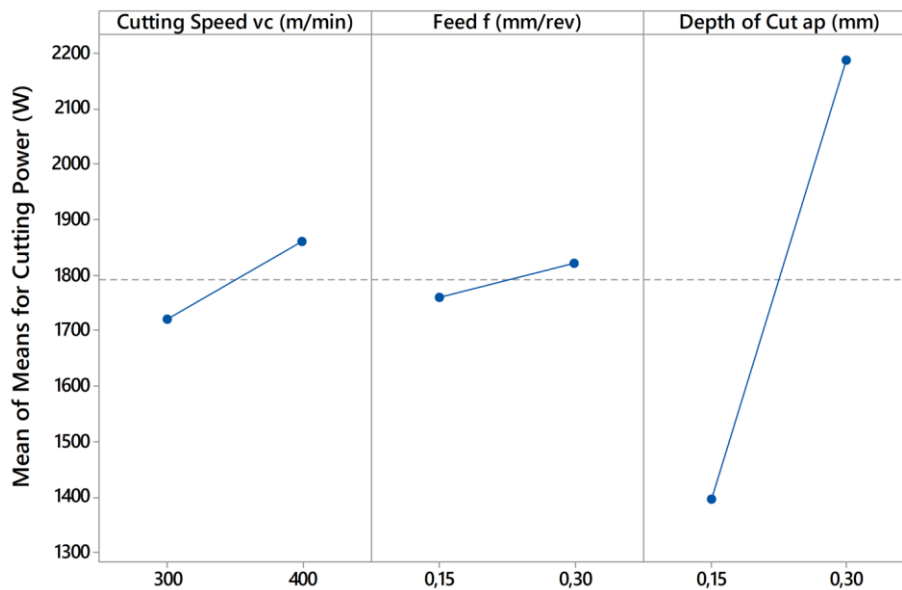


Figure 1. Main effect plots for cutting power.

Analyzing the main effect plot, the combination of variables resulted in the lowest cutting power was  $v_c = 300$  m/min,  $f = 0.15$  mm/rev and  $a_p = 0.15$  mm. The mean of means for cutting power found during the experiments was 1792.00 W.

The analysis of variance (ANOVA), using a confidence interval of 95% ( $\alpha = 0.05$ ), showed that the cutting speed (p-value = 0.002) and the depth of cut (p-value = 0,000) displayed a statistic difference in cutting power to different levels of the factor. The Percentage Contribution Rate (PCR) of the cutting speed was 2.94% and the PCR for depth of cut was 91,36%. Changing the level of the factor  $f$  did not show any statistic difference in power response.

The value of adjusted R-square was 98.18%, meaning that the model describes a high precision of behavior of cutting power during the experiment.

The Kolmogorov-Smirnov Normality test was done to assure the normality of the residuals. The p-value was greater than 0.15 assuring the normality of the residuals.

On the Tabel 4 it is shows the ANOVA analysis for cutting power.

Tabel 4. ANOVA analysis for cutting power (W)

Source	D.F.	Adj SS	Adj MS	F-Value	P-Value	PCR
$v_c$	1	121169	121169	14.06	0.002	2.94%
$f$	1	21307	21307	2.47	0.135	0.52%
$a_p$	1	3760021	3760021	436.23	0.000	91.36%
$v_c \times f$	1	30623	30623	3.55	0.078	0.74%
$v_c \times a_p$	1	27331	27331	3.17	0.094	0.66%
$f \times a_p$	1	1409	1409	0.16	0.691	0.03%
$v_c \times f \times a_p$	1	15816	15816	1.83	0.194	0.38%
Error	16	137910	8619			3.35%
Total	23	4115585				R-Sq (adj) = 98.18 %

PCR – Percentage Contribution Rate

Increased cutting speed and depth of cut lead to increased power consumption during cutting. As for the depth of cut, an increase in its value leads to an increase in the chip's thickness, therefore, it is needed that the machining center provides more power to operate. The difference between the high and low levels was 143 W. When compared to the power of the machining center, that difference represented less than 0.95% of the power available.

### 3.2 R<sub>a</sub> and R<sub>t</sub>

On the Figure 2 it is showed the main effects obtained for superficial roughness R<sub>a</sub> and in the Figure 3 is showed the interaction plot between the factors.

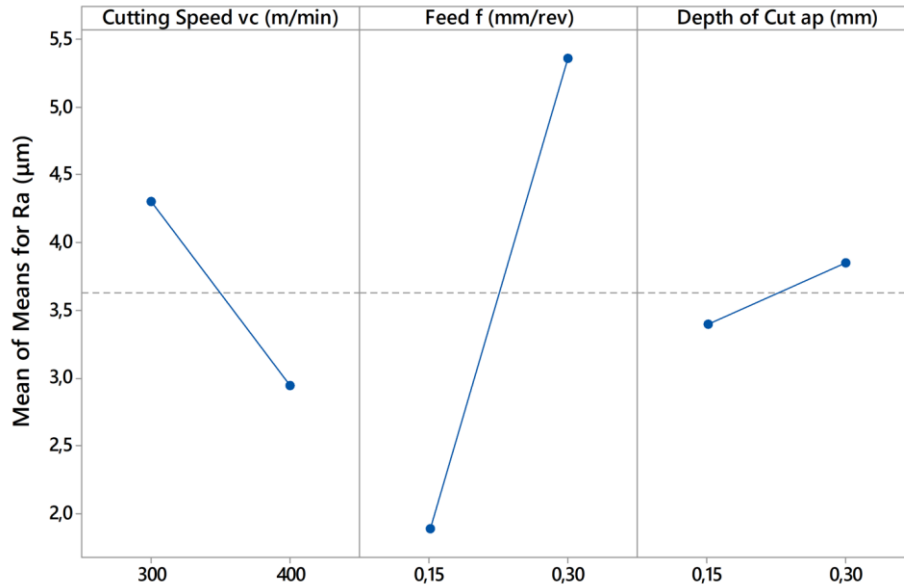


Figure 2. Main effect plots for R<sub>a</sub>.

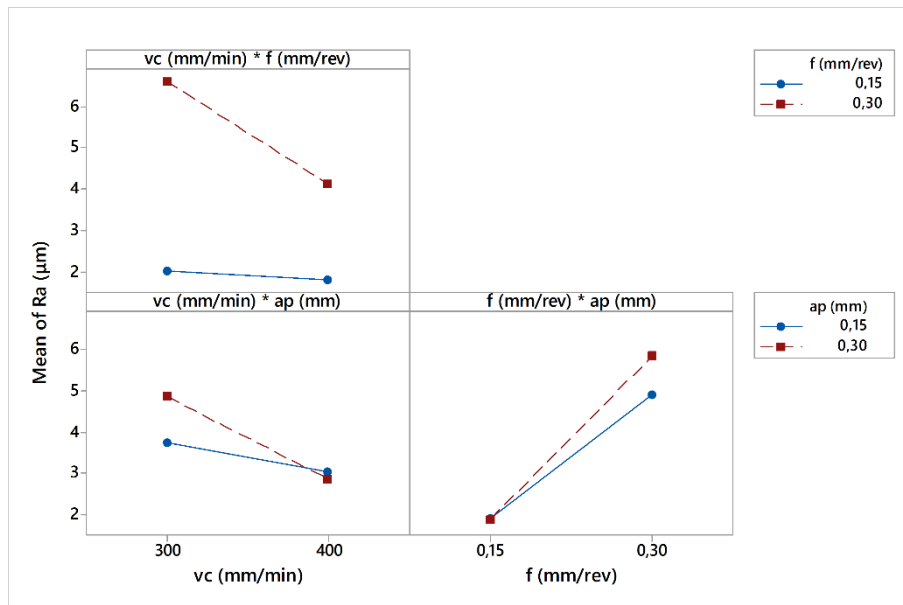


Figure 3. Interaction effect plots for R<sub>a</sub>.

According to the main effect analysis, the combination of factors that resulted in the lowest value of R<sub>a</sub> are  $v_c = 400$  m/min,  $f = 0.15$  mm/rev and  $a_p = 0.15$  m. The mean of means of R<sub>a</sub> found in the experiment was 3.628 µm.

In the ANOVA analysis, the factors that showed statistical significance were the cutting speed (p-value = 0.015), the feed (p-value = 0.000) and the interaction between the cutting speed and the feed (p-value = 0.032). The PCR for those factors were 9.12 %, 60.78 % and 6.69 %, respectively. The adjusted R-square for R<sub>a</sub> was 72.05%, therefore it is possible to state that the model describes with precision the behavior of R<sub>a</sub>.

On the table 5 is showed the ANOVA analysis for R<sub>a</sub>.

Tabel 5. ANOVA analysis for  $R_a$  ( $\mu\text{m}$ )

Source	D.F.	Adj SS	Adj MS	F-Value	P-Value	PCR
$v_C$	1	10.943	10.943	7.5	0.015	9.12%
$f$	1	72.934	72.934	49.71	0.000	60.78%
$a_p$	1	1.279	1.279	0.88	0.363	1.07%
$v_C \times f$	1	8.028	8.028	5.5	0.032	6.69%
$v_C \times a_p$	1	2.493	2.493	1,71	0.210	2.08%
$f \times a_p$	1	1.345	1.345	0.92	0,510	1.12%
$v_C \times f \times a_p$	1	0.098	0.098	0.07	0.799	0.08%
Error	16	23.335	1.458			19.45%
Total	23	120,005				R-Sq (adj) = 72.05 %

On the Tabel 6 it is shows the ANOVA analysis  $R_t$ .

Tabel 6. ANOVA analysis for  $R_t$  ( $\mu\text{m}$ )

Source	D.F.	Adj SS	Adj MS	F-Value	P-Value	PCR
$v_C$	1	398.88	398.88	15.57	0.001	15.40%
$f$	1	1331.88	1331.88	51.99	0.000	51.43%
$a_p$	1	70.63	70.63	2.76	0.116	2.73%
$v_C \times f$	1	73.98	73.98	2.89	0.109	2.86%
$v_C \times a_p$	1	27.47	27.47	1.07	0.316	1.06%
$f \times a_p$	1	227.65	227.65	8.89	0.009	8.79%
$v_C \times f \times a_p$	1	49.26	49.26	1.92	0.185	1.90%
Error	16	409.91	25.619			15.83%
Total	23	2589.65				R-Sq (adj) = 77.55 %

On the Figure 4 it is showed the mean effect plots for surface roughness  $R_t$  and in the Figure 3 is showed the interaction plot between the factors.

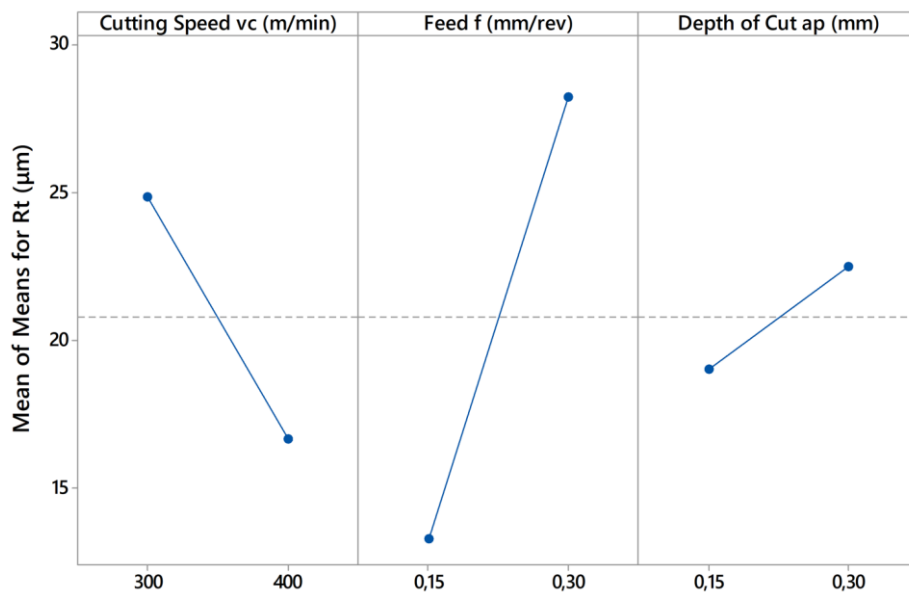


Figure 4. Main effect plots for  $R_t$ .

In the Figure 5 it is showed the interaction effect plots for surface roughness  $R_t$ .

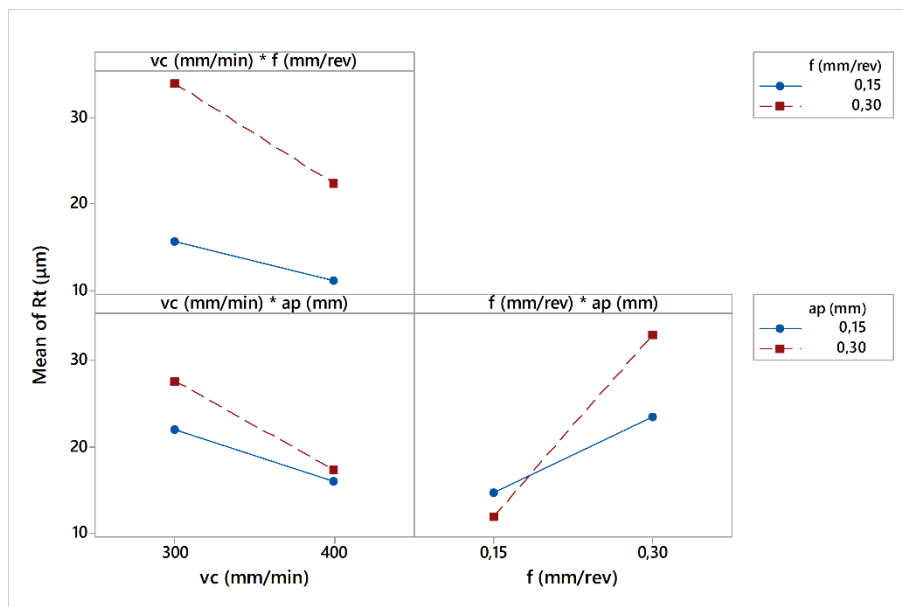


Figure 5. Interaction effect plots for  $R_t$ .

Regarding to the  $R_t$ , the ANOVA analysis found the factors that presented statistical significance were the cutting speed (p-value = 0.001), the feed (p-value = 0.000) and the interaction between the feed and the depth of cut (p-value = 0.009). The PCR for those factors were 15.40 %, 51.43 % and 8.79%, respectively.

The combination of parameters that results in lower values of  $R_t$  are  $v_c = 400$  m/min,  $f = 0.15$  mm/rev and  $a_p = 0.15$  m. The mean of means of  $R_t$  found in the experiment was  $20.76 \mu\text{m}$ . The interaction between the feed and the depth of cut produces the lesser value with  $f = 0.15$  and  $a_p = 0.30$  mm. However, this level of  $a_p$  produces the biggest values in cutting power. The Kolmogorov-Smirnov Normality test was done to assure the normality of the residuals of  $R_a$  and  $R_t$ . The p-value was greater than 0.150 in both responses, assuring the normality of the residuals.

To determine the optimal conditions for the Al<sub>2</sub>O<sub>3</sub>-MgO-based tool it was consider the roughness as the main factor on this paper. Therefore, the combination of parameters that produces the lesser values of surface roughness  $R_a$  and  $R_t$  are  $v_c = 400$  m/min,  $f = 0.15$  mm/rev and  $a_p = 0.15$  m

The surface roughness is highly influenced by the feed, as the feed increases the spacing between the cutting groves, it also increases resulting in a surface with more roughness. Regarding to the cutting speed, the increase of its values produced a better surface finish, i.e., smaller values of  $R_a$  and  $R_t$  and this conclusion is in accordance with the works of Thakur and Gangopadhyay (2015) and Vishwanatah *et al.* (2019), that concluded that the higher values of cutting speeds

results in better surface finish and the work of Kondo *et al.* (2018) that concluded the higher cutting speed and lesser feed and depth of cut results in better surface quality.

#### 4. CONCLUSION

The process of turning the superalloy VAT80A<sup>®</sup> with experimental ceramic tool was satisfactory in regarding the cutting power and the surface roughness. The optimal parameters for the Al<sub>2</sub>O<sub>3</sub>-MgO-based tool found in this paper was  $v_C = 400$  m/min,  $f = 0.15$  mm/rev and  $a_p = 0.15$  m.

#### 5. ACKNOWLEDGEMENTS

The authors would like to thank CAPES and CNPq for the financial aid, Villares Metals for donating the VAT 80A<sup>®</sup> and SECO TOOLS<sup>™</sup> for the partnership.

#### 6. REFERENCES

- Associação Brasileira de Normas Técnicas. Geometrical product specifications (GPS) - Surface texture: Profile method - Rules and procedures for the assessment of surface texture. Rio de Janeiro, 2002.
- Bonhin, E. P.; David-Müzel, S.; Souza, J. V. C.; Alves, M. C. S.; Ribeiro, M. V., 2019. "Effect of machining parameters on turning of VAT32<sup>®</sup> superalloy with ceramic tool". *Materials and Manufacturing Processes*, 34:7, 800-806, 2019, DOI: 10.1080/10426914.2019.1594261.
- Choudhury, I.; El-Baradie, M. 1998. "Machinability of Nickel-Base Super Alloys: A General Review". *J. Mater. Process. Technol.*, 77 (1-3), 278-284. DOI: 10.1016/S0924-0136(97)00429-9.
- Ezugwu, E. O. 2005. "Key Improvements in the Machining of Difficult-to-Cut Aerospace Superalloys." *International Journal of Machine Tools and Manufacture*. 45(12-13), 1353-1367. DOI: 10.1016/j.ijmachtools.2005.02.003.
- Farina, A. B., Liberto, R. C. N., Barbosa, C. A. 2013. "Desenvolvimento de novos aços válvula para aplicação em motores de alto desempenho." *Tecnologia em Metalurgia, Materiais e Mineração*, v10, p329, - 335.
- Kondo, M. Y., Pinheiro, C., Souza, J. V. C., Ribeiro, M. V., Alves, M. C.S. 2018. "Optimizing cutting parameters for cutting power and roughness in VAT 32<sup>®</sup> turning with an experimental Al<sub>2</sub>O<sub>3</sub> using Taguchi's method." *In 8th CIRP Conference on High Performance Cutting (HPC 2018)*, v77, p610-613,2018.
- Souza, T. A., 2020. "Usinagem de ferro fundido vermicular com ferramenta de corte à base de alumina magnésio." Tese (doutorado) - Universidade Estadual Paulista "Júlio de Mesquita Filho", Faculdade de Engenharia, Guaratinguetá, 2020. Print. 142 f.
- Thakur, A.; Gangopadhyay, S. 2016. "State-of-the-art in surface integrity in machining of nickel-based super alloys." *International Journal of Machine Tools and Manufacture*, v100, p25-64
- Vishwanath C., Shirish K., Mudigonda. 2019. "Performance of alumina-based ceramic inserts in high-speed machining of nimonic 80A." *Materials and Manufacturing Processes*, 34:1, 8-17, 2019. DOI: 10.1080/10426914.2018.1532084

#### 7. RESPONSIBILITY NOTICE

The authors are the only responsible for the printed material included in this paper.